Materials Today Bio 23 (2023) 100843

Contents lists available at ScienceDirect

Materials Today Bio

journal homepage: www.journals.elsevier.com/materials-today-bio

Mussel-inspired cortical bone-adherent bioactive composite hydrogels promote bone augmentation through sequential regulation of endochondral ossification

Shuyi Tan [a,1], Yonghao Qiu [a,1], Huacui Xiong [a], Chunhui Wang [a], Yifan Chen [a], Wangxi Wu [a], Zhen Yang [b,*], Fujian Zhao [a,**]

[a] Stomatological Hospital, School of Stomatology, Southern Medical University, Guangzhou, 510280, China
[b] Center for Health Science and Engineering, Hebei Key Laboratory of Biomaterials and Smart Theranostics, School of Health Sciences and Biomedical Engineering, Hebei University of Technology, Tianjin, 300131, China

ARTICLE INFO

Keywords:
Bioactive glass
Dopamine
Hydrogel
Endochondral ossification
Bone augmentation

ABSTRACT

Endochondral ossification (ECO) plays an integral part in bone augmentation, which undergoes sequential processes including mesenchymal stem cells (MSC) condensation, chondrocyte differentiation, chondrocyte hypertrophy, and mineralized bone formation. Thus, accelerating these steps will speed up the osteogenesis process through ECO. Herein, inspired by the marine mussels' adhesive mechanism, a bioactive glass-dopamine (BG-Dopa) hydrogel was prepared by distributing the micro-nano BG to aldehyde modified hyaluronic acid with dopamine-modified gelatin. By *in vitro* and *in vivo* experiments, we confirm that after implanting in the bone augmentation position, the hydrogel can adhere to the cortical bone surface firmly without sliding. Moreover, the condensation and hypertrophy of stem cells were accelerated at the early stage of ECO. Whereafter, the osteogenic differentiation of the hypertrophic chondrocytes was promoted, which lead to accelerating the late stage of ECO process to achieve more bone augmentation. This experiment provides a new idea for the design of bone augmentation materials.

1. Introduction

Alveolar ridges undergo sustained atrophy after natural teeth loss [1–3]. The severely atrophic alveolar ridge could not provide enough bone for tooth implantation [1–4]. With the increasing demand of dental implant treatment, the reconstruction of atrophic alveolar ridge becomes very urgent [5]. Autologous bone transplantation is the gold standard for bone augmentation [6]. However, its application is limited because of the donor site morbidity, unpredictable resorption, limited available quantities, and need for another surgical sites, which may increase the risk of complications not limited to pain, trauma and infection [6,7].These deficiencies can be avoided by using biomaterials in place of autologous bone grafts [8]. Our previous studies have found that Bioactive Glass (BG) could promote osteogenesis at the bone augmentation position without destroying the cortical bone [9–11]. BG promotes osteogenesis by dissolving bioactive ions, which shows osteoinductivity and has become a research hotspot in recent years. However, using BG for bone augmentation alone requires a long time.

By observing the bone tissue sections in our previous studies, we found that the osteogenesis process at bone augmentation position was endochondral ossification (ECO). ECO undergoes sequential processes including MSC condensation, chondrocyte differentiation, chondrocyte hypertrophy, and mineralized bone formation [12,13]. Among these steps, MSC condensation is the initiation step of chondrogenic differentiation. And then, ECO undergoes chondrocyte hypertrophy, which is an important step because it means the ECO process switch from chondrogenesis to osteogenesis [14]. Thus, accelerating these steps will significantly speed up the osteogenesis process through ECO. BG has been widely reported to promote osteogenic differentiation [15–17], but its effect on the early stage of ECO remains unclear. This problem can be solved by adding components which promote the early process of ECO such as promoting cell condensation, chondrogenic differentiation and

* Corresponding author.
** Corresponding author.
E-mail addresses: yangzhenqdu@163.com (Z. Yang), zhaofj@smu.edu.cn (F. Zhao).
[1] These authors contributed equally to this work.

https://doi.org/10.1016/j.mtbio.2023.100843
Received 9 July 2023; Received in revised form 11 October 2023; Accepted 22 October 2023
Available online 25 October 2023

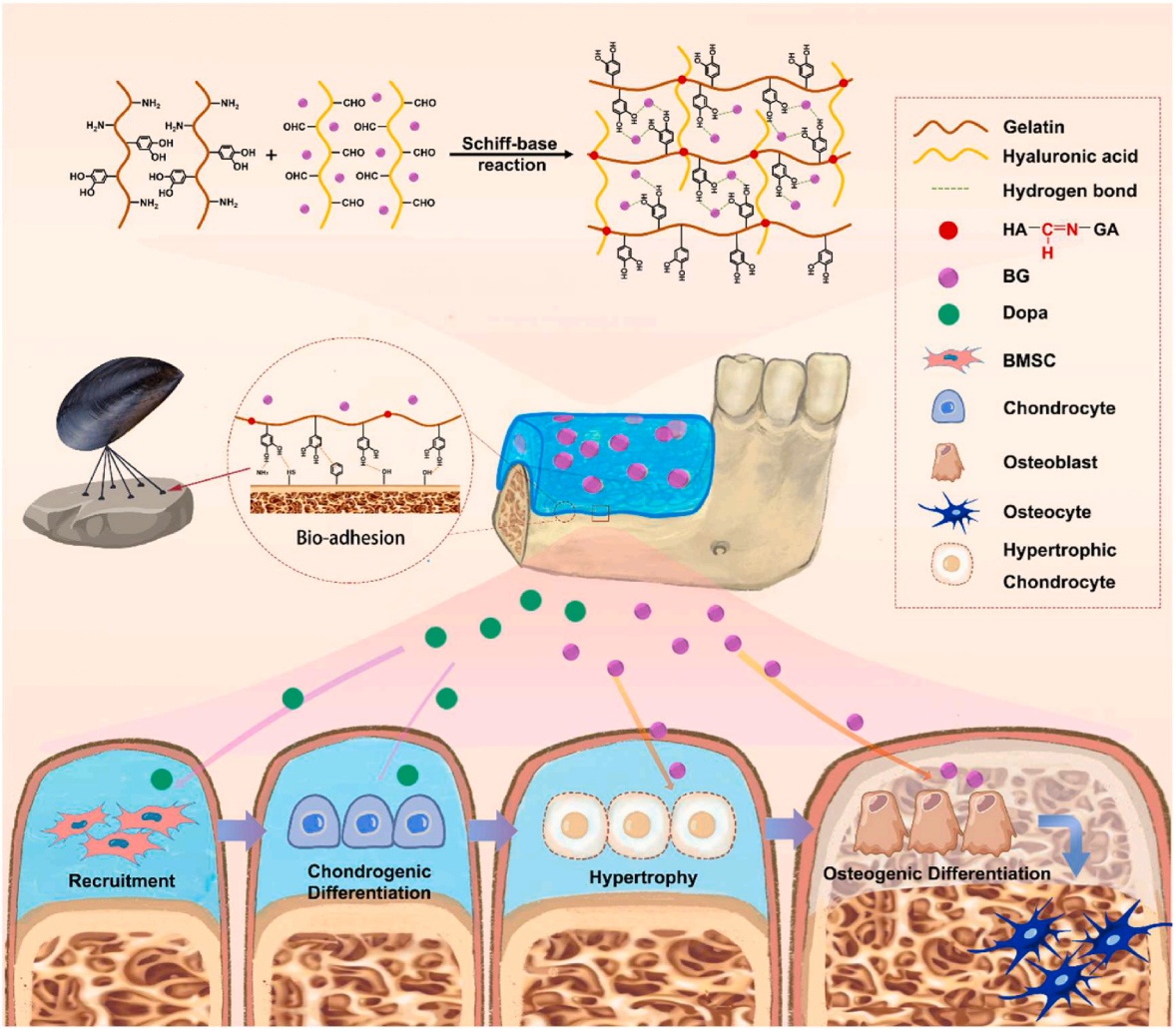

Fig. 1. Schematic illustration. Inspired by marine mussels' adhesive mechanism, a BG-Dopa hydrogel was fabricated, which was based on the Schiff-base reaction by micro-nano BG distributed aldehyde modified hyaluronic acid with dopamine-modified gelatin. After implanting into the bone augmentation area, the BG-Dopa hydrogel adhered to the bone firmly and promoted the process of ECO sequentially to achieve bone augmentation.

hypertrophic in bone augmentation materials. Dopamine is widely used in cartilage repair. As a modified component of cartilage repair scaffolds, dopamine promotes the recruitment of stem cells [18] and cell cluster/condensation [19]. The cell recruitment leads to an increase in local cell density, which in turn increases cell-cell interaction and lead to condensation [20,21]. The high density of BMSC and promotion of cell-cell interaction [20,22]/condensation [22] are conducive to chondrogenic differentiation [23]. Since the recruitment of stem cells, the cell condensation and the formation of cartilage matrix are important steps of ECO, dopamine has the potential to accelerate the early process of ECO. Among the markers used to evaluate chondrocyte hypertrophy and ECO, RUNX2, OCN, OPN, and ALP have been confirmed to be upregulated by BG [24–28]. Thus, it is speculated that DOPA-promoted early process of ECO is likely to result in hypertrophy under the synergistic effect of BG. Therefore, the combination of BG and dopamine to construct composite bone augmentation material is expected to sequentially accelerate the steps of ECO process in bone augmentation position.

In addition, besides rapid osteogenesis and shortened osteogenesis cycle, the space creation and its maintenance during healing are essential. Also, the stabilization of the grafting material is the key to success [29]. Because the surface of atrophic alveolar ridge crest is mostly convex [1], it is difficult for the biomaterials to fix in place, and the displacement of bone graft material results in bone augmentation failure [29]. Therefore, it is necessary to add adhesion components to the bone augmentation material to stabilize it at the bone increment site. Coincidentally, dopamine is an analogue of L-3,4-dihydroxyphenylalanine (Dopa), which mediates underwater robust adhesion of mussels, and the adhesive application of dopamine has become a focus of research in recent years [30,31]. Therefore, the combination of dopamine is expected to bond the material to the bone augmentation site firmly. However, bone augmentation with dopamine has not been reported.

Therefore, in this experiment, a BG-dopamine (BG-Dopa) hydrogel was prepared by distributing the BG to hyaluronic acid with dopamine-modified gelatin. The mechanical property, adhesion property and biocompatibility of the BG-Dopa hydrogel were tested. More importantly, the sequential progress of ECO by the dopamine and BG were verified and the chondrogenic hypertrophic mechanism was analyzed.

2. Materials and methods

2.1. Synthesis and characterization of BG-Dopa hydrogel

The micro-nano BG, aldehyde modified hyaluronic acid and dopamine-modified gelatin was prepared according to our previous reported [32,33] and the experimental procedures are showed in the supplementary data. To prepare the micro-nano BG distributed aldehyde

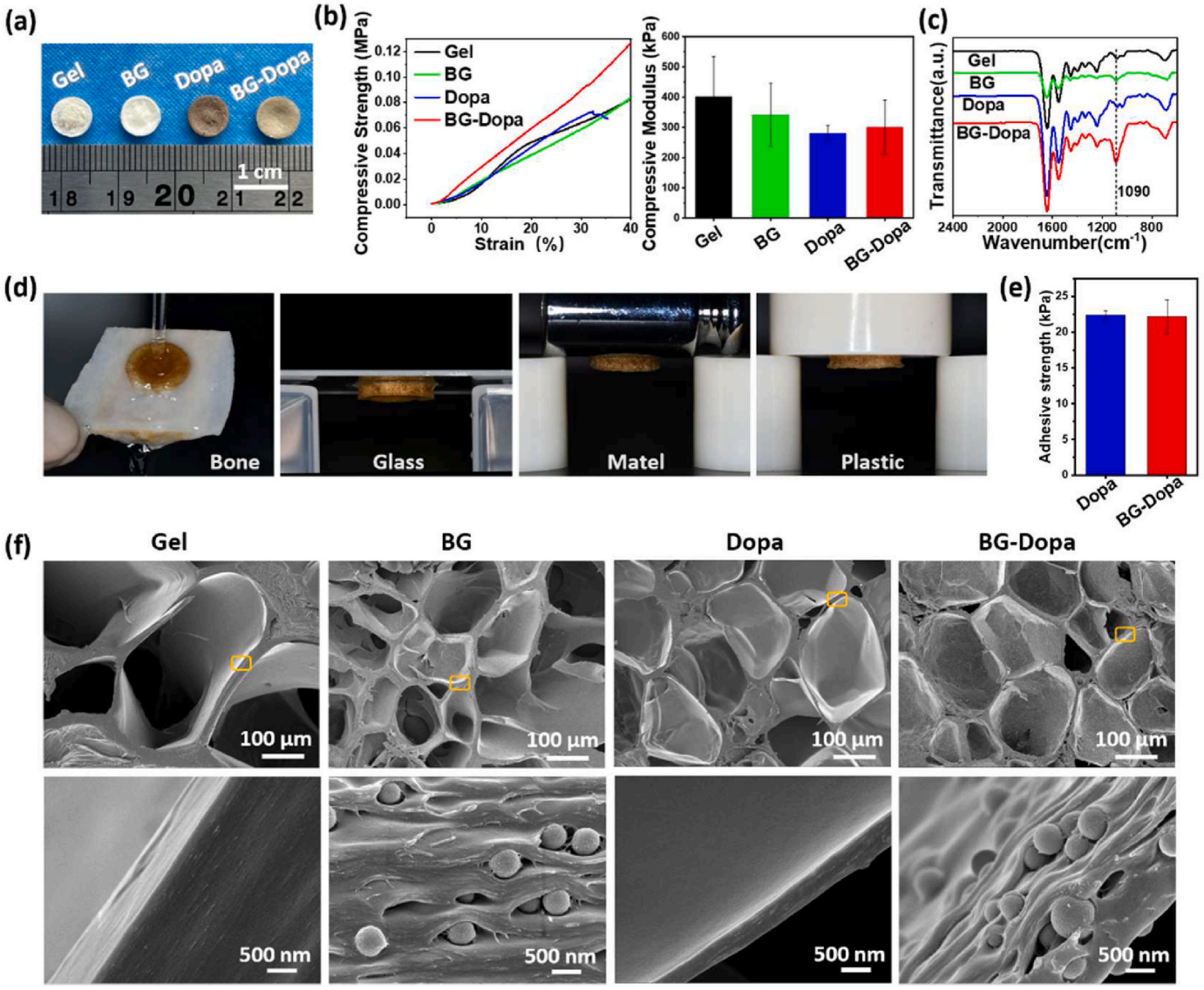

Fig. 2. Physical characteristics of Gel, BG, Dopa and BG-Dopa hydrogels. (a) The digital photograph of the hydrogels. (b) The compressive strength and compressive modulus of the hydrogels. (c) FTIR spectra of hydrogels. (d) Adhesion of the BG-Dopa hydrogel to bone tissue and different materials. (e) Adhesion strength to bone tissue of Dopa and BG-Dopa hydrogels. (f) SEM images of the hydrogels at different magnifications.

modified hyaluronic acid, 0.1 g BG powder was added into 2.5 mL deionized water for ultrasonic dispersion. Then, 0.5 g of aldehyde modified hyaluronic acid was added into the above BG dispersion liquid and stirred until completely dissolved. Meanwhile, 0.75 g dopamine-modified gelatin (or unmodified gelatin) was dissolved in 2.5 mL deionized water and stirred at 60° centigrade until it was dissolved and heated to return to room temperature.

At this point, the gelatin solution (with or without dopamine-modified) and the hyaluronic acid solution (with or without micro-nano BG distributed) were done. After that, gelatin solution was mixed with hyaluronic acid solution and stirred at room temperature for 10 min. The evenly mixed precursor solution was injected into the mold and stood at 4° centigrade for 10 min so that the mold could be released smoothly. After that, the hydrogel was lyophilized to dehydrated.

Through the above-mentioned approach, four tissue engineering scaffolds were done, which respectively were the Gel hydrogel (containing hyaluronic acid with gelatin), the BG hydrogel (containing BG distributed hyaluronic acid with gelatin), the Dopa hydrogel (containing hyaluronic acid with dopamine-modified gelatin), and the BG-Dopa hydrogel (containing BG distributed hyaluronic acid with dopamine-modified gelatin).

To detecting the surface morphology and composition, SEM and FTIR was used to evaluate the BG-freeze-drying Dopa hydrogel. And then, the mechanical properties were observed by testing the compressive strength of BG-Dopa with cylindrical hydrogel (5 mm high × 10 mm diameter) on the universal mechanical tester (Instron, USA). After calibration and zeroing, the hydrogel was pressed at the rate of 1 mm/min until the hydrogel sheet was broken. After that, the adhesion of the hydrogels to bone tissue and different materials were tested. To evaluate the adhesion of BG-Dopa hydrogel to bone, the hydrogel was placed between two cow bones for a few minutes, and the bonding strength of the hydrogel was tested using a universal testing machine (Instron, USA).

2.2. *In vitro biocompatibility test of BG-Dopa hydrogel*

The hydrogel was placed in 75 % alcohol, irradiated by ultraviolet light overnight to remove bacteria, rinsed with Dulbecco's Modified Eagle's Medium (DMEM; Gibco, USA) containing 10 % fetal bovine serum (FBS; Gibco, USA) for 3 times (1 h each time) to replace the

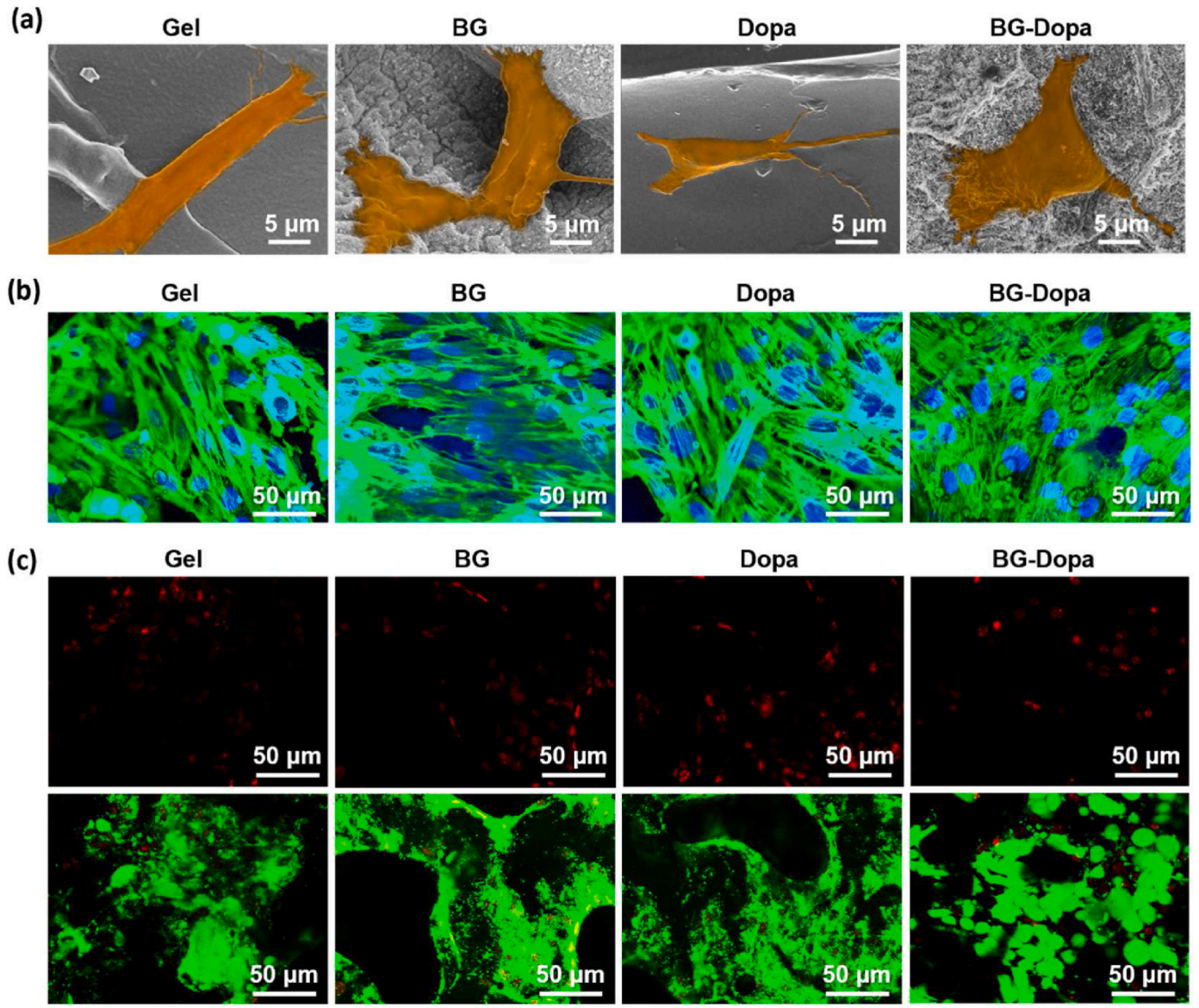

Fig. 3. Cytocompatibility of mBMSCs on the hydrogels. (a) SEM images of mBMSCs on the hydrogels. (b) Cytoskeleton staining of mBMSCs on the hydrogels for 72 h. (c) Live/dead staining of mBMSCs on the hydrogels for 72 h. Green indicates the live cells, and red indicates the dead cells. (For interpretation of the references to color in this figure legend, the reader is referred to the Web version of this article.)

remaining alcohol, and the hydrogel was placed in a 48-well plate for use. The mouse bone marrow-derived mesenchymal stromal cells (mBMSCs) (Cyagen, China) that had grown to 80 % fusion were digested with trypsin (Gibco, USA). mBMSCs (1×10^6 cells per well) was seeded into hydrogels in the 48-well plate. After 72 h of culture, cytoskeletal staining and live/dead staining was performed. The fluorescence was visualized using a laser scanning confocal microscope (Leica STELLARIS 5, Germany).

2.3. *In vitro cell condensation/hypertrophy and mechanism analysis*

To obtain the enzymatic hydrolysate of the hydrogel scaffold, type I collagenase (100 μg/mL) was added into the DMEM contains a hydrogel scaffold, which was degraded on a constant temperature shaking bed (37 °C, 120 rpm) for about 6 h until the hydrogel was completely dissociated. The bacteria were filtered by a 0.22 μm filter for later use. Subsequently, the enzymatic hydrolysate was used for the following *in vitro* experiments. The effects of the enzymatic hydrolysate for cell proliferation were studied by CCK-8.

To investigate the cell condensation of the BG-Dopa hydrogel, high-density micromass culture for mBMSCs were used. The high-density micromass culture was an *in vitro* model of endochondral skeletal development, in which the chondrocytes from MSCs showed favorable ability for hypertrophic differentiation, and calcification occurred sequentially [34]. Previous research has shown that it is a convenient *in vitro* model to investigate the regulatory mechanisms of endochondral ossification [35,36]. In brief, the mBMSCs were seeded in 24-well plates at high density (1.5×10^7 cells/mL). Add chondrogenic medium which contained Gel, BG, Dopa and BG-Dopa enzymatic hydrolysate and incubate for 6 days. The medium was replaced every 48–72 h. At day 4 and day 6, cells were visualized with inverted microscope (Observer7, Zeiss, Germany) and captured. At day 6, bioinformatic analysis and RNA sequencing (RNA-seq) were done to investigate the hypertrophic mechanism of BG-Dopa. After that, immunohistochemical staining was done to analyze the expression of collagen type X. The protein expressions of N-cadherin and SOX9 were analyzed by western-blot.

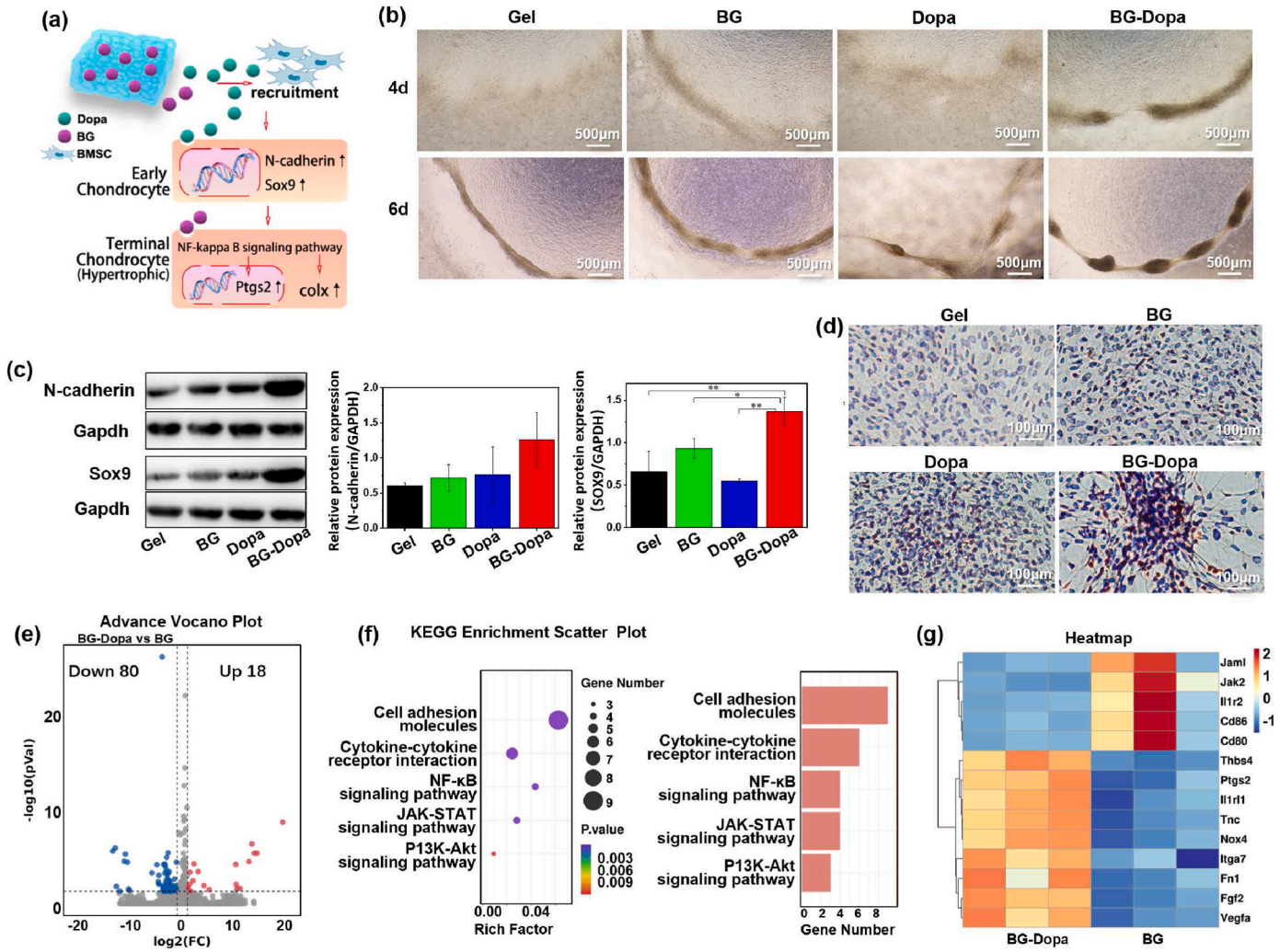

Fig. 4. Hypertrophy properties and mechanism. (a) Schematic illustration of chondrogenesis mechanism. (b) Images of live mBMSCs under light microscope with chondrogenic incubation at day 4 and day 6. (c) Western-blot analysis and relative protein expression of N-cadherin and SOX9 at day 6. (*$p < 0.05$, **$p < 0.01$) (d) Immumohistochemical staining of collagen type X at day 6. (e) Volcano plot of the differentially expressed genes between BG-Dopa and BG groups. (log2FC ≥ 1 & q < 0.05; red: upregulated genes; blue: downregulated genes). (f) The gene enrichment KEGG pathways analysis of BG-Dopa vs BG. (g) Heat map of Chondrogenic differentiation and hypertrophy related gene expression in BG-Dopa compared to BG. (For interpretation of the references to color in this figure legend, the reader is referred to the Web version of this article.)

2.4. In vitro osteogenic differentiation assessment

After 6 days of chondrogenic induction, the mBMSCs were then switched to osteogenic induction medium which contained Gel, BG, Dopa and BG-Dopa enzymatic hydrolysate and incubated for another 14 days. At day 1 and day 7 of osteogenic induction, cells were visualized with inverted microscope and captured. At day 14, the osteogenic differentiation of cells was studied by Alizarin Red staining and ALP staining. Three control holes were selected from each group of samples, and semi-quantitative analysis of alizarin red staining was performed using image J software. The protein expressions of OPN were analyzed by western-blot.

2.5. In vivo ECO and bone augmentation evaluation

All the 32 rats were purchased from the animal experiment center of Guangzhou Pharmaceutical University. The experimental procedures were performed in accordance with the Institutional Animal Care of Guangdong Pharmaceutical University. To minimize pain and discomfort to the animals, measurements were taken such as adequate anesthesia.

To evaluate the osteogenic properties, Gel, BG, Dopa and BG-Dopa hydrogels were transplanted into Sprague Dawley rats (SD rats, male, 200–250 g) following the bone augmentation animal model previously described [37]. Briefly, 32 rats were randomly divided into four groups. After anesthesia by intraperitoneal injection of pentobarbital (Nembutal, 3.5 mg/100 g), a 15 mm incision was made on the scalp following by turning over the mucoperiosteal flap to form a pocket. Gel, BG, Dopa and BG-Dopa hydrogels with a thickness of 2 mm and diameter of 6 mm was inserted to the pocket under the periosteum on the surface of cortical bone without bone defect, which was then closed by suture. With unrestricted mobility and routine feeding for 3 and 6 weeks, an overdose of sodium pentobarbital was used to sacrifice the rats. The hydrogels together with the surrounding skull were cut off and soaked in 4 % paraformaldehyde solution for 12 h. Micro-CT (XTV160H, X-TEK Co., UK) was taken to detect the bone augmentation area with 60 kV voltage and 67 mA current, and the minimum resolution was 25 × 25 × 25 μm. Three-dimensional images were reconstructed based on the CT data to examine the new bone volume.

Subsequently, the skulls were decalcified for 4 weeks, and then the bone tissue sections were prepared. Masson's staining, Movat staining, safranin O-fast green staining and immumohistochemical staining of

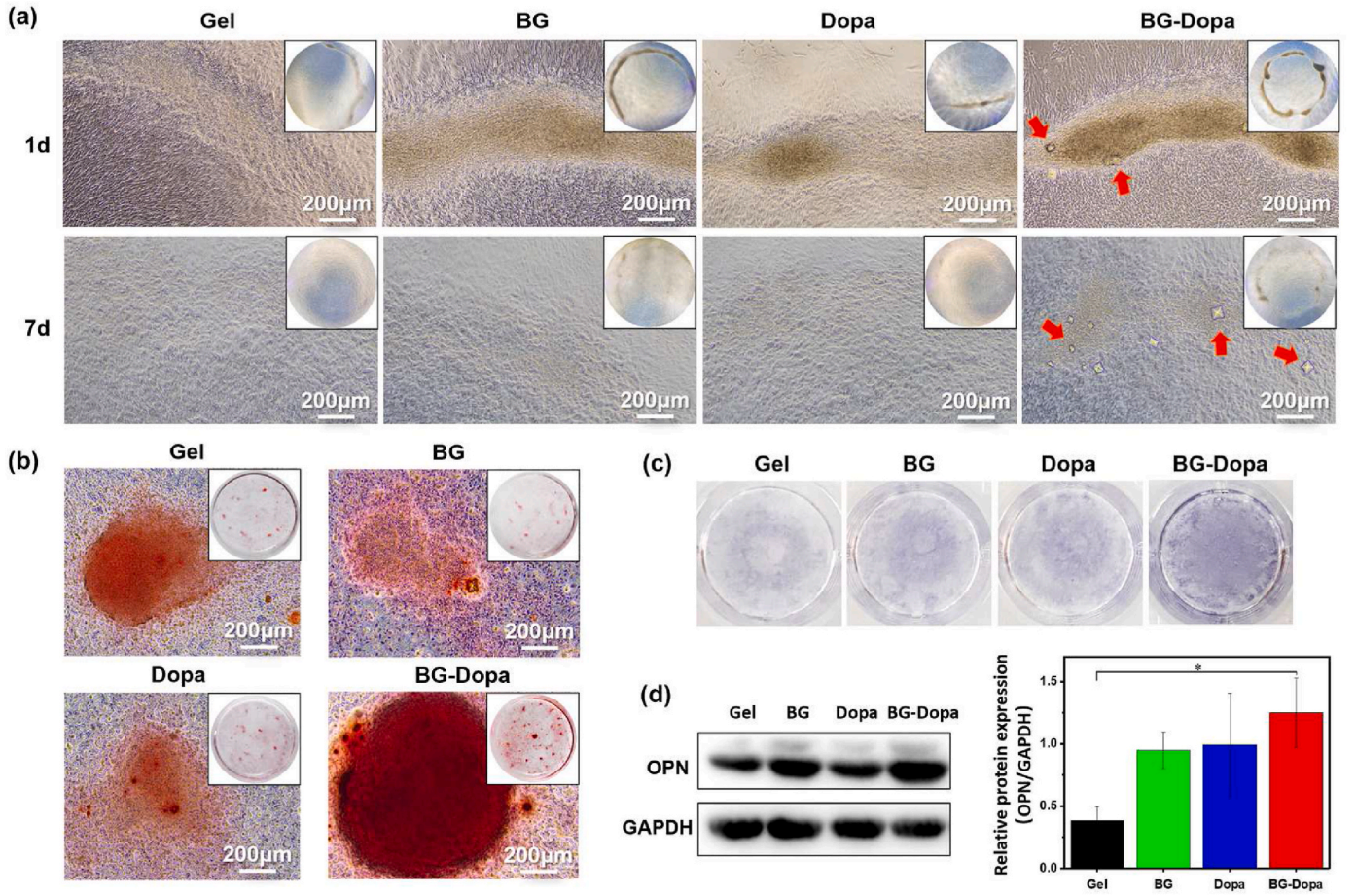

Fig. 5. Osteogenesis properties. (a) Images of live mBMSCs with osteogenic induced incubation at day 1 and day 7. (b) Alizarin red staining at day 14. (c) ALP staining at day 14. (d) Western-blot analysis of OPN expression at day 14. (*$p < 0.05$). (For interpretation of the references to color in this figure legend, the reader is referred to the Web version of this article.)

Collagen X and OPN were performed. A digital pathological scanning system (Aperio ImageScope, Zeiss, Germany) was used to scanned and photographed the sections.

2.6. Statistical analysis

All quantitative experiments were performed in triplicate and the data were presented as means ± standard deviation. Student's *t*-test or one-way analysis was conducted using Origin version 2021. $p < 0.05$ was considered significant.

3. Results

3.1. Preparation and characteristics of BG-Dopa hydrogels

In this experiment, a dopamine-modified gelatin-hyaluronic acid hydrogel containing micro-nano BG was fabricated (Figs. 1 and 2a). The two components of this reaction are dopamine-modified gelatin and the aldehyde modified hyaluronic acid solution [33]. After that, the –CHO on hyaluronic acid reacts with the amino group on the gelatin through Schiff base reaction to form a cross-linked network and preserved the activity of the dopamine group at the same time.

Hydrogen bonds can be formed between the –OH of catechol on GA-Dopa, and between the GA-Dopa and the –OH of Si on the surface of BG, which further enhances the stability of the composite hydrogel. Then, the chemical bond of composite hydrogels was identified by FTIR. In the BG-Dopa group, with the addition of BG, change of the spectrum in at ~1082 cm^{-1} was detected attributed to the asymmetric stretching vibration peak of Si–*O*–Si. The FTIR (Fig. 2c) results combined with the SEM image (Fig. 2f) showed that BG was evenly distributed to the surface and interior of the hydrogel. The compressive strength in the BG-Dopa group was higher within 30–40 % because of the addition of BG, and the difference between the compressive modulus of each group was not obvious (Fig. 2b). Through the modification of dopamine, the hydrogel in this experiment can be bonded to the bone, glass, metal, and polytetrafluoroethylene (Fig. 2d). In addition, the adhesive strength of the BG-Dopa hydrogel (22.2 ± 2.4 kPa) was not affected by the doping of BG by detecting the adhesive strength as quantitative analysis has no significant difference compared to Dopa hydrogels (Fig. 2e). All these results confirmed that BG-Dopa exhibits excellent adhesive properties and compressive resistance to meet the requirements of bone augmentation materials.

To test the biocompatibility of BG-Dopa hydrogel, mBMSCs were seeded into hydrogels in the 48-well plate and co-culture for 72 h. SEM images revealed differing mBMSCs morphologies and attachment on the surface of all the hydrogels. mBMSCs seeded into the BG and BG-Dopa hydrogels exhibited multiple tentacles morphology, intense growth and spreading (Fig. 3a). Furthermore, the cytoskeleton and live/dead staining and CCK-8 was done to detect the biocompatibility of the BG-Dopa hydrogel. The hydrogels allowed the adhesion and spreading of mBMSCs and only a few dead cells were observed after 72 h of co-culture (Fig. 3 b-c). Quantification of the cell number in cytoskeleton staining showed that there was no statistical difference among the four groups (Fig. S2 a). Fig. S2b showed that in the BG-Dopa group, the number of living cells was 31.8 ± 5.0 times that of dead cells and there was no statistical difference among the four groups. In addition, the CCK-8

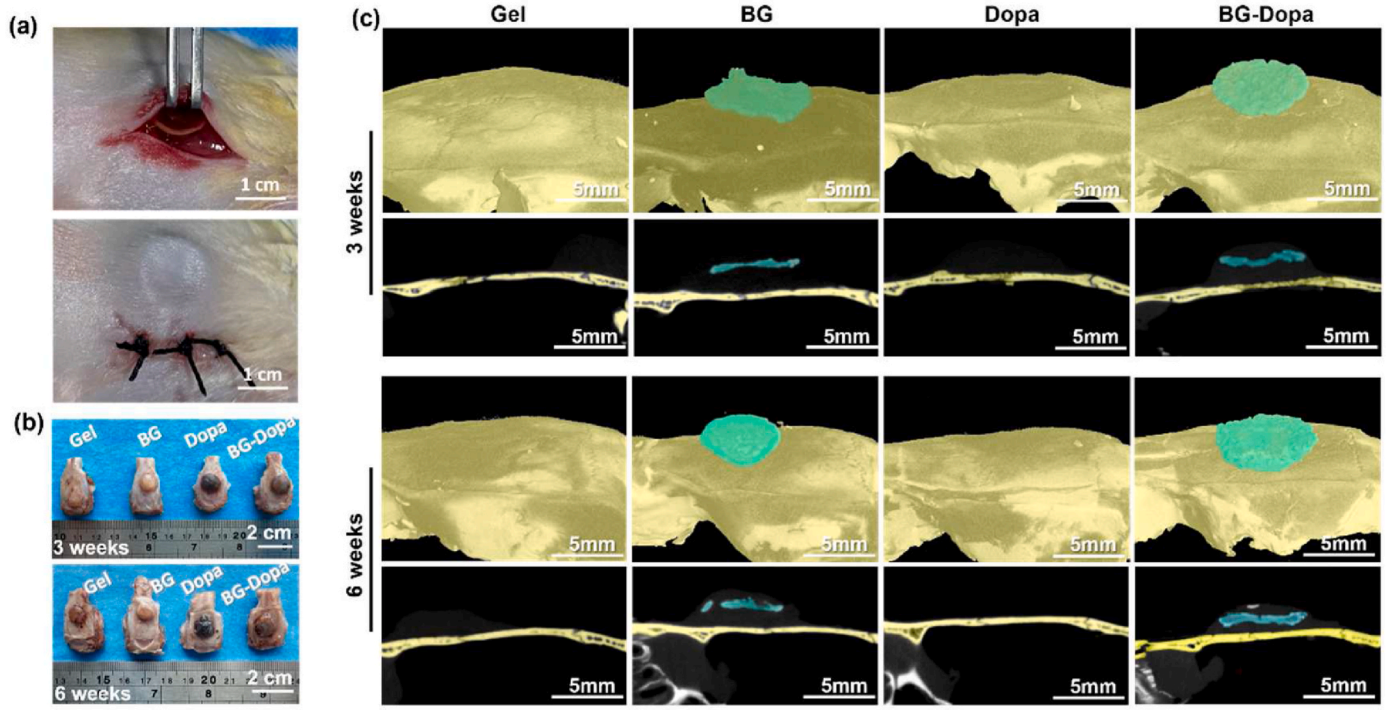

Fig. 6. *In vivo* new bone formation evaluation at 3 and 6 weeks. (a) Surgical incision and sutures. (b) Skull samples at 3 and 6 weeks. (c) 3D reconstruction images of hydrogels and surrounding tissue by Micro-CT including side view and section view. The green color refers to the new immature bone tissue. (For interpretation of the references to color in this figure legend, the reader is referred to the Web version of this article.)

assay was employed and showed that there was no adverse effect on mBMSCs' proliferation incubated with the enzymatic hydrolysate of the BG-Dopa hydrogel (Fig. S2 c).

3.2. *In vitro cell condensation and hypertrophic properties and mechanism of BG-Dopa hydrogels*

The result of this section indicated that mBMSCs in the BG-Dopa group showed condensation, chondrogenic differentiation and hypertrophic trend. Chondrocytes derive in embryogenesis from multipotent skeletal progenitor cells, as do osteoblasts. When RUNX2 and OSX is highly expressed, the multipotent skeletal progenitor cells differentiated into osteoblasts. When SOX9 in highly expressed, the multipotent skeletal progenitor cells differentiated into pre-chondrocytes, early chondrocytes, and terminal chondrocytes sequentially. After differentiating into terminal chondrocytes, the cells become hypertrophic and the expression of SOX9 becomes decline [38]. With high density seeding, the cell-cell junctions of mBMSCs enhanced, which resulted in high expression of N-cadherin. When the hypertrophy occurred in the late stage of MSCs chondrogenesis, the N-cadherin expression decreased [39] and the collagen type X expression increased [40]. The expression of type X collagen is restricted to hypertrophic chondrocytes in regions undergoing endochondral ossification [41]. After 4 days of treatment of mBMSCs with chondrogenic induction medium prepared by hydrogel enzymatic hydrolysate, cell recruitment differences began to appear in each group (Fig. 4b). In the BG-Dopa group, there were obvious cell high-density clumps at day 4, and cells were further recruited to string-of-beads at day 6 to show condensation. Western-blot showed that the expression of SOX9 protein enhanced in the BG-dopa group, while the relative mRNA expression was not statistically significant (Fig. S1). The expression of N-cadherin protein was not statistically significant (Fig. 4c). In addition, collagen type X was significantly increased in the BG-Dopa group by immunohistochemical staining (Fig. 4d). The above results indicated that mBMSCs in the BG-Dopa group showed condensation, chondrogenic differentiation and hypertrophic trend.

To further investigate the mechanism of BG-Dopa promoting hypertrophy of mBMSCs, RNA-seq was done. Compared with the BG group, eighty genes were down regulated, and eighteen genes were up regulated in the BG-Dopa group (Fig. 4e). KEGG enrichment scatter plot showed that several signal pathways are associated with cartilage formation, among which NF-κB signal pathway is related to cartilage hypertrophy (Fig. 4f). The up-regulated Ptgs2 (also known as Cox-2) in Heat map is related to cartilage hypertrophy (Fig. 4g). All the above results showed that dopamine promoted the condensation and chondrogenic differentiation of mBMSCs, and the mBMSCs went through hypertrophy under the synergistic effect of BG (Fig. 4a).

3.3. *In vitro osteogenesis properties of BG-Dopa hydrogels*

After 1 day of osteogenic induction, mineralized crystals could be observed at a 20-fold microscope in BG-Dopa group, and the cells still showed high-density clumps (Fig. 5a). At the 7th day of osteogenic induction, the number and size of mineralized crystals in BG-Dopa group were further increased, significantly more than those in the other 3 groups, and the black high-density clumps were no longer obvious (Fig. 5a). After 14 days of osteogenic induction, the alizarin red and ALP staining was significantly darker in the BG-Dopa group (Fig. 5b and c). Statistical analysis of alizarin red staining results showed that BG-Dopa group had significant statistical difference with the other three groups ($p < 0.001$) (Fig. S3). The osteopontin (OPN) protein expression was higher in the BG-Dopa group (Fig. 5d), indicating that the BG-Dopa group had the best mineralization effect.

In summary, the BG-Dopa hydrogel could sequentially promote ECO by promoting chondrogenic induction differentiation in the early stage, and promote osteogenic induction differentiation in the late stage.

3.4. *In vivo ECO and bone augmentation of BG-dopa hydrogels*

New bone formation of Gel, BG, Dopa and BG-Dopa hydrogel was conducted *in vivo* for 3 and 6 weeks. By taking the skull samples, it was

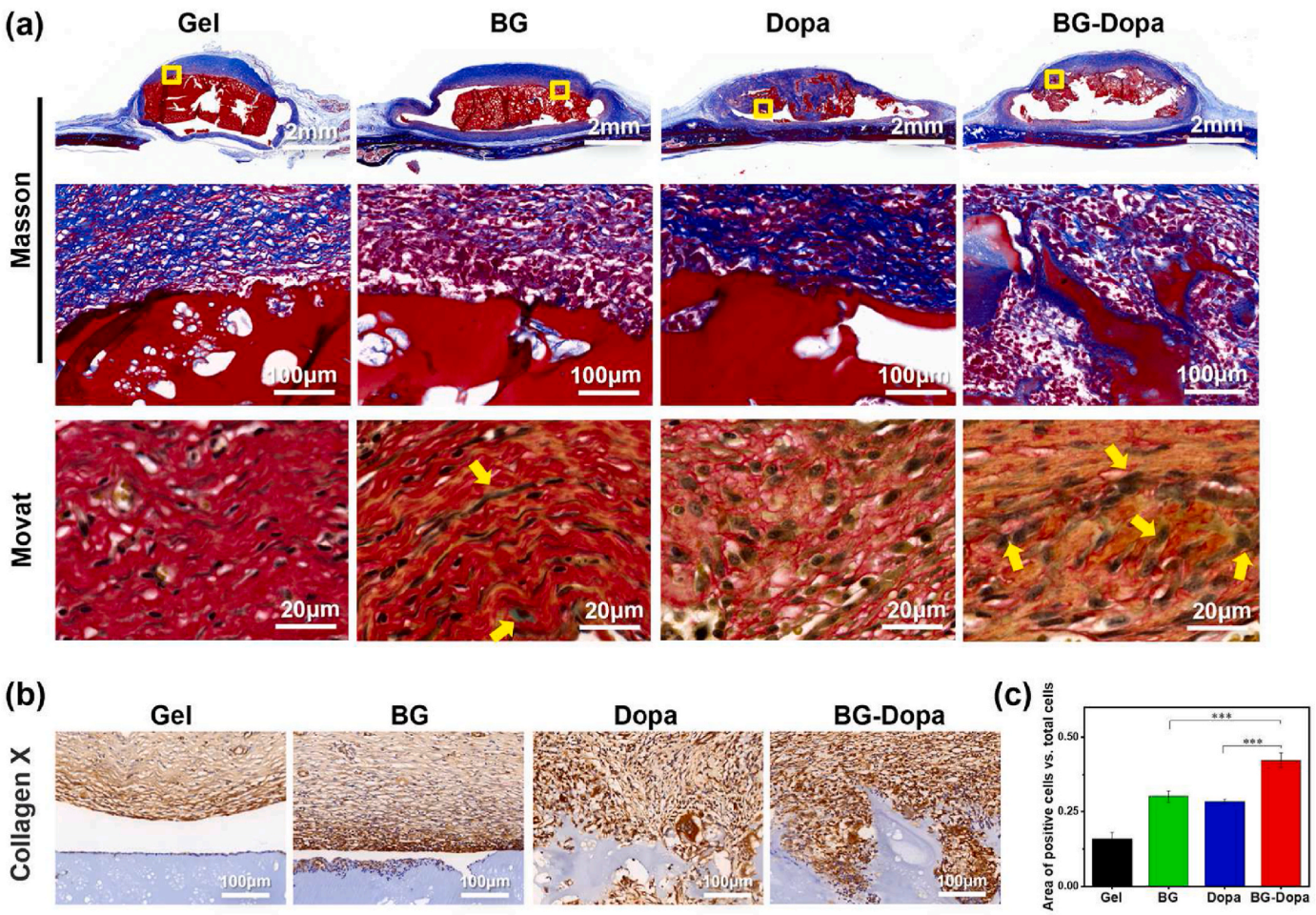

Fig. 7. Histologic sections and staining at 3 weeks. (a) Masson and Movat staining. (b) Immumohistochemical staining of Collagen X at 20×. (c) The area rate of Collagen X positive cells in total cells by immumohistochemical staining. (***$p < 0.001$).

found that the Dopa group and the BG-Dopa group were adhered firmly to the cortical bone surface at 3 weeks (Video. S1). At 6 weeks, all four groups were tightly bound to bone tissue. However, obvious tissue collapse occurred in Gel group and Dopa group. The longitudinal section of skull sample showed that the bone graft area in the Gel and Dopa group was collapsed due to premature degradation. Subsequently, micro-CT scanning was performed. It was found that at 6 weeks, the osteogenic effect was more obvious than that of at 3 weeks. At 6 weeks, bone formation in the BG-Dopa group was better than that in the BG group (Fig. 6c).

The skull samples were made into histologic sections and stained. At 3 weeks, Masson's staining, Movat staining and immumohistochemical staining of Collagen X were performed (Fig. 7). Hydrogel in each group had been partially degraded at 3 weeks in Masson staining. Compared with the other three groups, the tissues around the BG-Dopa hydrogel showed "invasive" growth, and there was no obvious smooth boundary between the tissues and the hydrogel. Hypertrophic chondrocytes were scattered in Movat stained sections in both BG group and BG-Dopa group, and more in the BG-Dopa group (Fig. 7a). Immumohistochemical staining showed that Collagen type X expressed higher in the BG-Dopa group (Fig. 7b and c) and the Collagen type II expressed higher in the Dopa and BG-Dopa groups (Fig. S4). The result is consistent with the early biological process of ECO.

At 6 weeks, Masson's staining, safranin O-fast green staining and immumohistochemical staining of OPN were performed (Fig. 8). The BG group and the BG-DOPA group showed better support. The Gel group and Dopa group showed obvious gap and collapse between the new tissues and hydrogels. The degradation of the BG group occurred mainly in the periphery of the hydrogel, while the BG-Dopa group showed uniform degradation around and in the center of the hydrogel. The "bony" tissue was more mature in the BG-Dopa group then in the other three groups in the safranin O and fast green staining (Fig. 8a). Immumohistochemical staining showed that OPN expressed higher in the BG-Dopa group (Fig. 8b and c). This is consistent with the late biological process of ECO.

4. Discussions

In this experiment, a dopamine-modified gelatin-hyaluronic acid hydrogel containing micro-nano BG was fabricated. Our research confirmed that BG-Dopa hydrogel can promote the process of ECO at the bone augmentation area.

Firstly, the *in vitro* experiment confirmed that the BG-Dopa hydrogel can promote recruitment, condensation and hypertrophy of mBMSCs. We performed a high-density micromass culture experiments with mBMSCs *in vitro*. After 4 days of chondrogenic induction, earlier of cell aggregation was observed under the microscope in BG-Dopa group, which confirmed that BG-Dopa could promote the recruitment of mBMSCs. The protein expression of N-cadherin was not statistically significant, which showed that the cell hypertrophy was not inhibited [39]. The expression of SOX9 protein enhanced in the BG-dopa group, while the mRNA expression was not statistically significant. SOX9 is highly expressed when the skeletal progenitors cells differentiate into chondrocytes, and it was inhibited when differentiate into terminal

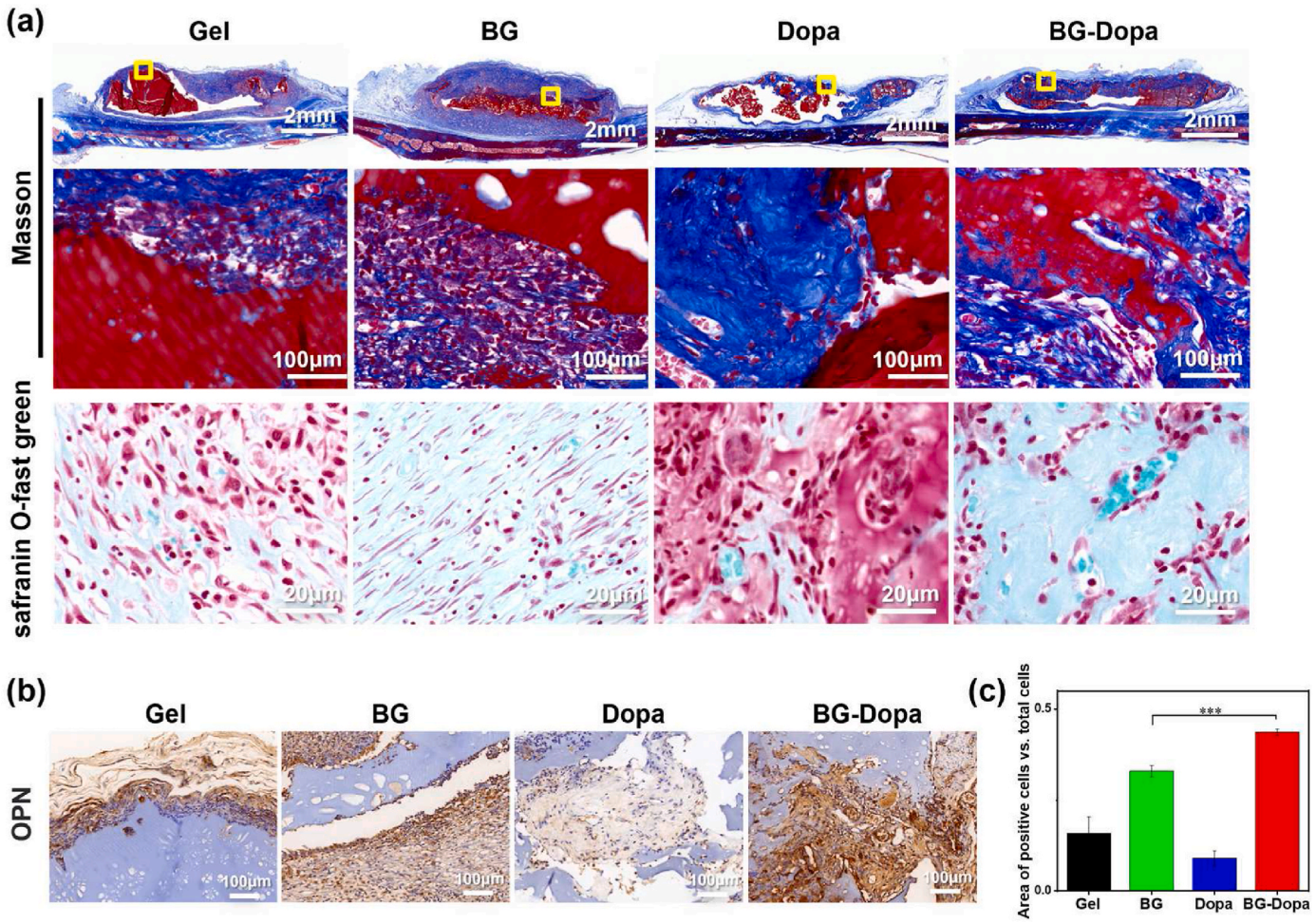

Fig. 8. Histologic sections and staining at 6 weeks. (a) Masson and safranin O-fast green staining. (b) Immumohistochemical staining of OPN. (c) The area rate of OPN positive cells in total cells by immumohistochemical staining. (***$p < 0.001$). (For interpretation of the references to color in this figure legend, the reader is referred to the Web version of this article.)

chondrocyte and osteoblasts [38]. It indicated that the cells in the BG-Dopa were differentiated from the early chondrocytes to terminal chondrocytes (hypertrophic). Ptgs2, a cytokine in NF-κB signaling pathway [42], is associated with the hypertrophy of chondrocytes [43,44], which is an important process of ECO. Meanwhile, high expression of collagen type X is essential for successful cartilage formation mediated by mesenchymal stem cell and subsequent endochondral ossification [45], and it could be up-regulated by activating the NF-κB signaling pathway [43,46]. Thus, it can be speculated that in the BG-Dopa group, the activation of NF-κB signaling pathway increased the expression of Ptgs2 and collagen type X. Therefore, increased of cell recruitment, secretion of cartilage-related collagen X, and hypertrophy of mBMSCs in the BG-Dopa group, confirmed that BG-Dopa hydrogel can promote the recruitment and hypertrophy process of ECO.

Secondly, we further confirmed that BG-Dopa hydrogel can promote the mineralization process of ECO *in vitro*. After 6 days of chondrogenic induction, the culture medium was then switched to osteogenic induction medium which contained Gel, BG, Dopa and BG-Dopa enzymatic hydrolysate and incubated for another 14 days. Meantime, significantly enhanced mineralization was observed in the BG-Dopa group. BG has been widely reported to promote osteogenic differentiation [15–17], which was mutually verified with our experimental results. It is worth noting that some mineralized crystals have been generated in the BG-Dopa group compared with the other three groups after osteogenic induction for 1 day. We speculated that BG played a role as the mineralization induction factor before the addition of osteogenic induction solution. Subsequently, with earlier cell recruitment, faster mineralization occurred in the effect of BG once switching into osteogenic induction solution. These results indicated that the ECO process was dynamic, during which the cells present sequential differentiation. Cells recruited earlier would undergo differentiation, hypertrophy and mineralization faster. These results also indicated in the bone tissue sections, in which the formation of bone tissue is also asynchronous.

Thirdly, we found that the BG-Dopa hydrogel had a better osteogenic effect after 6 weeks of implantation *in vivo*. Our previous studies have found that BG forms new bone without destroying cortical bone at the bone increment site [37]. In this study, we used this innovative experimental model for bone augmentation. Our study showed that the BG-Dopa hydrogel attached to the skull firmly and had sufficient support for the bone graft area. This is important for the successful clinical application of scaffolds for bone tissue engineering [29,47]. In addition, the bone formation in the BG-Dopa group was better than that in the other three groups. We found that compared with the other three groups, the tissues around the BG-Dopa hydrogel showed "invasive" growth, and there was no obvious boundary between the tissues and the hydrogel. This confirms that the BG-Dopa hydrogel has osteoconductivity [48]. At 3 weeks' histologic sections, hypertrophic chondrocytes were scattered in Movat stained sections, and Collagen type X expressed higher in the BG-Dopa group. At 6 weeks' histologic sections, the "bony" tissue was more mature and the OPN expressed higher in the BG-Dopa group. This confirms that the BG-Dopa hydrogel has osteoinductivity [48,49]. The results *in vivo* are consistent with the *in vitro*

findings in this study.

From the above mentions, we indicated that once the BG-Dopa hydrogel was implanted in the bone augmentation area, the scaffold can be stably fixed to the surface of the cortical bone. And then, with the synergistic effect of Dopa and BG, the mBMSCs went through condensation, chondrogenic differentiation and hypertrophy. In this process, the expressions of SOX9 and N-cadherin were up-regulated first and then down-regulated. Meanwhile, the hypertrophic markers including Ptgs2 and collagen type X were up-regulated, which may be resulted from the activation of NF-κB signaling pathway. Then, the BG could enhance the process of ossification, which may finally lead to promoting the ECO.

5. Conclusion

Inspired by the key steps of ECO, a dopamine-modified gelatin-hyaluronic acid hydrogel containing BG was successfully prepared. After implanting in the bone augmentation position, the hydrogel can adhere to the cortical bone surface firmly without sliding. And then, the condensation and hypertrophy of stem cells at the early stage of ECO were accelerated. Whereafter, the osteogenic differentiation of the hypertrophic chondrocytes was promoted, which lead to accelerating the late stage of ECO process to achieve more bone augmentation. This experiment provides a new idea for the design of bone augmentation materials.

Credit author statement

Shuyi Tan: Methodology, Formal analysis, Writing-original draft preparation, Writing-review & editing. Yonghao Qiu: Methodology, Formal analysis, Writing-Original draft reparation. Huacui Xiong: Formal analysis, Technical supports. Chunhui Wang: Software, Technical supports. Yifan Chen, Wangxi Wu: Conceptualization, Technical supports. Zhen Yang: Project administration, Conceptualization, Writing-review. Fujian Zhao: Writing-review & editing, Supervision, Project administration, Funding acquisition.

Declaration of competing interest

The authors declare the following financial interests/personal relationships which may be considered as potential competing interests: Fujian Zhao reports financial support was provided by National Natural Science Foundation of China, China and Young Talent Support Project of Guangzhou Association for Science and Technology, China.

Data availability

Data will be made available on request.

Acknowledgements

This work was supported by the National Natural Science Foundation of China (No. 32171311, 32000933), the Young Talent Support Project of Guangzhou Association for Science and Technology (No. QT-2023-020).

Appendix A. Supplementary data

Supplementary data to this article can be found online at https://doi.org/10.1016/j.mtbio.2023.100843.

References

[1] E. Couso-Queiruga, S. Stuhr, M. Tattan, L. Chambrone, G. Avila-Ortiz, Post-extraction dimensional changes: a systematic review and meta-analysis, J. Clin. Periodontol. 48 (1) (2021) 126–144.

[2] F. Van der Weijden, F. Dell'Acqua, D.E. Slot, Alveolar bone dimensional changes of post-extraction sockets in humans: a systematic review, J. Clin. Periodontol. 36 (12) (2009) 1048–1058.

[3] K. Hayashi, M. Shimabukuro, R. Kishida, A. Tsuchiya, K. Ishikawa, Structurally optimized honeycomb scaffolds with outstanding ability for vertical bone augmentation, J. Adv. Res. 41 (2022) 101–112.

[4] G. Avila-Ortiz, S. Elangovan, K.W. Kramer, D. Blanchette, D.V. Dawson, Effect of alveolar ridge preservation after tooth extraction: a systematic review and meta-analysis, J. Dent. Res. 93 (10) (2014) 950–958.

[5] I.A. Urban, M.H.A. Saleh, A. Ravidà, A. Forster, H.L. Wang, Z. Barath, Vertical bone augmentation utilizing a titanium-reinforced PTFE mesh: a multi-variate analysis of influencing factors, Clin. Oral Implants Res. 32 (7) (2021) 828–839.

[6] C.E. Gillman, A.C. Jayasuriya, FDA-approved bone grafts and bone graft substitute devices in bone regeneration, Mater. Sci. Eng., C 130 (2021), 112466.

[7] G.J. McKenna, H. Gjengedal, J. Harkin, N. Holland, C. Moore, M. Srinivasan, Effect of autogenous bone graft site on dental implant survival and donor site complications: a systematic review and meta-analysis, J. Evid. Base Dent. Pract. 22 (3) (2022), 101731.

[8] R. Tevlin, A. McArdle, D. Atashroo, G.G. Walmsley, K. Senarath-Yapa, E.R. Zielins, K.J. Paik, M.T. Longaker, D.C. Wan, Biomaterials for craniofacial bone engineering, J. Dent. Res. 93 (12) (2014) 1187–1195.

[9] F. Zhao, W. Xie, W. Zhang, X. Fu, W. Gao, B. Lei, X. Chen, 3D printing nanoscale bioactive glass scaffolds enhance osteoblast migration and extramembranous osteogenesis through stimulating immunomodulation, Adv. Healthcare Mater. 7 (16) (2018), e1800361.

[10] F. Zhao, B. Lei, X. Li, Y. Mo, R. Wang, D. Chen, X. Chen, Promoting in vivo early angiogenesis with sub-micrometer strontium-contained bioactive microspheres through modulating macrophage phenotypes, Biomaterials 178 (2018) 36–47.

[11] F. Zhao, Z. Yang, H. Xiong, Y. Yan, X. Chen, L. Shao, A bioactive glass functional hydrogel enhances bone augmentation via synergistic angiogenesis, self-swelling and osteogenesis, Bioact. Mater. 22 (2023) 201–210.

[12] E. Kozhemyakina, A.B. Lassar, E. Zelzer, A pathway to bone: signaling molecules and transcription factors involved in chondrocyte development and maturation, Development 142 (5) (2015) 817–831.

[13] S.C. Dennis, C.J. Berkland, L.F. Bonewald, M.S. Detamore, Endochondral ossification for enhancing bone regeneration: converging native extracellular matrix biomaterials and developmental engineering in vivo, Tissue Eng., Part B 21 (3) (2015) 247–266.

[14] R. Fu, C. Liu, Y. Yan, Q. Li, R.L. Huang, Bone defect reconstruction via endochondral ossification: a developmental engineering strategy, J. Tissue Eng. 12 (2021), 20417314211004211.

[15] M. Chen, F. Zhao, Y. Li, M. Wang, X. Chen, B. Lei, 3D-printed photoluminescent bioactive scaffolds with biomimetic elastomeric surface for enhanced bone tissue engineering, Mater. Sci. Eng., C 106 (2020), 110153.

[16] W. Zhang, D. Huang, F. Zhao, W. Gao, L. Sun, X. Li, X. Chen, Synergistic effect of strontium and silicon in strontium-substituted sub-micron bioactive glass for enhanced osteogenesis, Mater. Sci. Eng., C 89 (2018) 245–255.

[17] P.S. Lee, C. Heinemann, K. Zheng, R. Appali, F. Alt, J. Krieghoff, A. Bernhardt, A. R. Boccaccini, U. van Rienen, V. Hintze, The interplay of collagen/bioactive glass nanoparticle coatings and electrical stimulation regimes distinctly enhanced osteogenic differentiation of human mesenchymal stem cells, Acta Biomater. 149 (2022) 373–386.

[18] Z. Li, H. Cao, Y. Xu, X. Li, X. Han, Y. Fan, Q. Jiang, Y. Sun, X. Zhang, Bioinspired polysaccharide hybrid hydrogel promoted recruitment and chondrogenic differentiation of bone marrow mesenchymal stem cells, Carbohydr. Polym. 267 (2021), 118224.

[19] D. Gan, Y. Jiang, Y. Hu, X. Wang, Q. Wang, K. Wang, C. Xie, L. Han, X. Lu, Mussel-inspired extracellular matrix-mimicking hydrogel scaffold with high cell affinity and immunomodulation ability for growth factor-free cartilage regeneration, J Orthop Translat 33 (2022) 120–131.

[20] H. Park, D. Kim, K.Y. Lee, Interaction-tailored cell aggregates in alginate hydrogels for enhanced chondrogenic differentiation, J. Biomed. Mater. Res. 105 (1) (2017) 42–50.

[21] C. Tacchetti, S. Tavella, B. Dozin, R. Quarto, G. Robino, R. Cancedda, Cell condensation in chondrogenic differentiation, Exp. Cell Res. 200 (1) (1992) 26–33.

[22] X. Yang, S. Tian, L. Fan, R. Niu, M. Yan, S. Chen, M. Zheng, S. Zhang, Integrated regulation of chondrogenic differentiation in mesenchymal stem cells and differentiation of cancer cells, Cancer Cell Int. 22 (1) (2022) 169.

[23] T.Y. Hui, K.M. Cheung, W.L. Cheung, D. Chan, B.P. Chan, In vitro chondrogenic differentiation of human mesenchymal stem cells in collagen microspheres: influence of cell seeding density and collagen concentration, Biomaterials 29 (22) (2008) 3201–3212.

[24] X. Liu, Z. Du, X. Yi, T. Sheng, J. Yuan, J. Jia, Circular RNA circANAPC2 mediates the impairment of endochondral ossification by miR-874-3p/SMAD3 signalling pathway in idiopathic short stature, J. Cell Mol. Med. 25 (7) (2021) 3408–3426.

[25] B. Dai, Y. Zhu, X. Li, Z. Liang, S. Xu, S. Zhang, Z. Zhang, S. Bai, W. Tong, M. Cao, Y. Li, X. Zhu, W. Liu, Y. Zhang, L. Chang, P.S. Yung, K. Ki-Wai Ho, J. Xu, T. Ngai, L. Qin, Blockage of osteopontin-integrin β3 signaling in infrapatellar fat pad attenuates osteoarthritis in mice, Adv. Sci. 10 (22) (2023), e2300897.

[26] E. Prado Ferraz, G. Pereira Freitas, M. Camuri Crovace, O. Peitl, E. Dutra Zanotto, P.T. de Oliveira, M. Mateus Beloti, A. Luiz Rosa, Bioactive-glass ceramic with two crystalline phases (BioS-2P) for bone tissue engineering, Biomed Mater 12 (4) (2017), 045018.

[27] N. Saffarian Tousi, M.F. Velten, T.J. Bishop, K.K. Leong, N.S. Barkhordar, G. W. Marshall, P.M. Loomer, P.B. Aswath, V.G. Varanasi, Combinatorial effect of Si4

+, Ca2+, and Mg2+ released from bioactive glasses on osteoblast osteocalcin expression and biomineralization, Mater. Sci. Eng., C 33 (5) (2013) 2757–2765.
[28] G.C. Reilly, S. Radin, A.T. Chen, P. Ducheyne, Differential alkaline phosphatase responses of rat and human bone marrow derived mesenchymal stem cells to 45S5 bioactive glass, Biomaterials 28 (28) (2007) 4091–4097.
[29] I.A. Urban, E. Montero, E. Amerio, D. Palombo, A. Monje, Techniques on vertical ridge augmentation: indications and effectiveness, Periodontol 2000 (2023), 10.1111.
[30] M. Renner-Rao, F. Jehle, T. Priemel, E. Duthoo, P. Fratzl, L. Bertinetti, M. J. Harrington, Mussels fabricate porous glues via multiphase liquid-liquid phase separation of multiprotein condensates, ACS Nano 16 (12) (2022) 20877–20890.
[31] Y. Li, J. Cheng, P. Delparastan, H. Wang, S.J. Sigg, K.G. DeFrates, Y. Cao, P. B. Messersmith, Molecular design principles of Lysine-DOPA wet adhesion, Nat. Commun. 11 (1) (2020) 3895.
[32] T. Tian, W. Xie, W. Gao, G. Wang, L. Zeng, G. Miao, B. Lei, Z. Lin, X. Chen, Micro-nano bioactive glass particles incorporated porous scaffold for promoting osteogenesis and angiogenesis in vitro, Front. Chem. 7 (2019) 186.
[33] Z. Yang, Z. Yang, L. Ding, P. Zhang, C. Liu, D. Chen, F. Zhao, G. Wang, X. Chen, Self-adhesive hydrogel biomimetic periosteum to promote critical-size bone defect repair via synergistic osteogenesis and angiogenesis, ACS Appl. Mater. Interfaces 14 (32) (2022) 36395–36410.
[34] X. Wang, T. He, L. He, B. Yang, Z. Liu, M. Pang, P. Xie, L. Zhang, L. Rong, Melatonin contributes to the hypertrophic differentiation of mesenchymal stem cell-derived chondrocytes via activation of the Wnt/β-catenin signaling pathway : melatonin promotes MSC-derived chondrocytes hypertrophy, Stem Cell Res. Ther. 12 (1) (2021) 467.
[35] T. Hayata, Y. Ezura, M. Asashima, R. Nishinakamura, M. Noda, Dullard/Ctdnep1 regulates endochondral ossification via suppression of TGF-β signaling, J. Bone Miner. Res. 30 (2) (2015) 318–329.
[36] M.A. Mello, R.S. Tuan, High density micromass cultures of embryonic limb bud mesenchymal cells: an in vitro model of endochondral skeletal development, In Vitro Cell. Dev. Biol. Anim. 35 (5) (1999) 262–269.
[37] F. Zhao, W. Xie, W. Zhang, X. Fu, W. Gao, B. Lei, X. Chen, 3D printing nanoscale bioactive glass scaffolds enhance osteoblast migration and extramembranous osteogenesis through stimulating immunomodulation, Adv. Healthcare Mater. 10 (20) (2021), e2101840.
[38] V. Lefebvre, M. Angelozzi, A. Haseeb, SOX9 in cartilage development and disease, Curr. Opin. Cell Biol. 61 (2019) 39–47.
[39] W. Ke, L. Ma, B. Wang, Y. Song, R. Luo, G. Li, Z. Liao, Y. Shi, K. Wang, X. Feng, S. Li, W. Hua, C. Yang, N-cadherin mimetic hydrogel enhances MSC chondrogenesis through cell metabolism, Acta Biomater. 150 (2022) 83–95.
[40] S. Gebhard, E. Pöschl, S. Riemer, E. Bauer, T. Hattori, H. Eberspaecher, Z. Zhang, V. Lefebvre, B. de Crombrugghe, K. von der Mark, A highly conserved enhancer in mammalian type X collagen genes drives high levels of tissue-specific expression in hypertrophic cartilage in vitro and in vivo, Matrix Biol. 23 (5) (2004) 309–322.
[41] M.L. Warman, M. Abbott, S.S. Apte, T. Hefferon, I. McIntosh, D.H. Cohn, J. T. Hecht, B.R. Olsen, C.A. Francomano, A type X collagen mutation causes Schmid metaphyseal chondrodysplasia, Nat. Genet. 5 (1) (1993) 79–82.
[42] S.C. Wong, M. Fukuchi, P. Melnyk, I. Rodger, A. Giaid, Induction of cyclooxygenase-2 and activation of nuclear factor-kappaB in myocardium of patients with congestive heart failure, Circulation 98 (2) (1998) 100–103.
[43] P. Lepetsos, K.A. Papavassiliou, A.G. Papavassiliou, Redox and NF-κB signaling in osteoarthritis, Free Radic. Biol. Med. 132 (2019) 90–100.
[44] T.J. Welting, M.M. Caron, P.J. Emans, M.P. Janssen, K. Sanen, M.M. Coolsen, L. Voss, D.A. Surtel, A. Cremers, J.W. Voncken, L.W. van Rhijn, Inhibition of cyclooxygenase-2 impacts chondrocyte hypertrophic differentiation during endochondral ossification, Eur. Cell. Mater. 22 (2011) 420–436, discussion 436-427.
[45] C.A. Knuth, E. Andres Sastre, N.B. Fahy, J. Witte-Bouma, Y. Ridwan, E. M. Strabbing, M.J. Koudstaal, J. van de Peppel, E.B. Wolvius, R. Narcisi, E. Farrell, Collagen type X is essential for successful mesenchymal stem cell-mediated cartilage formation and subsequent endochondral ossification, Eur. Cell. Mater. 38 (2019) 106–122.
[46] C. Nakatomi, M. Nakatomi, T. Matsubara, T. Komori, T. Doi-Inoue, N. Ishimaru, F. Weih, T. Iwamoto, M. Matsuda, S. Kokabu, E. Jimi, Constitutive activation of the alternative NF-κB pathway disturbs endochondral ossification, Bone 121 (2019) 29–41.
[47] P.K. Moy, T. Aghaloo, Risk factors in bone augmentation procedures, Periodontol. 2000 81 (1) (2019) 76–90.
[48] H.H. Xu, P. Wang, L. Wang, C. Bao, Q. Chen, M.D. Weir, L.C. Chow, L. Zhao, X. Zhou, M.A. Reynolds, Calcium phosphate cements for bone engineering and their biological properties, Bone Res 5 (2017), 17056.
[49] Y. Li, X. Zhang, C. Dai, Y. Yin, L. Gong, W. Pan, R. Huang, Y. Bu, X. Liao, K. Guo, F. Gao, Bioactive three-dimensional graphene oxide foam/polydimethylsiloxane/zinc silicate scaffolds with enhanced osteoinductivity for bone regeneration, ACS Biomater. Sci. Eng. 6 (5) (2020) 3015–3025.